J. CHEM. SOC. FARADAY TRANS., 1995, 91(8), 1261–1266

Effect of Tetrahedral Ti in Titania–Silica Mixed Oxides on Epoxidation Activity and Lewis Acidity

Seiichiro Imamura* and Tohru Nakai
Department of Chemistry, Kyoto Institute of Technology, Matsugasaki, Sakyo-ku, Kyoto 606, Japan
Hiroyoshi Kanai
Faculty of Life Science, Kyoto Prefectural University, Shimogamo, Sakyo-ku, Kyoto 606, Japan
Tomoyasu Ito
School of Social Information Studies, Otsuma Women's University, Karakida, Tama, Tokyo 206, Japan

The states of Ti in titania–silica mixed oxides have been studied by varying the Ti content. EXAFS analyses indicated that the amount of tetrahedral Ti species increased with a decrease in the Ti content reaching a maximum at 10 to 20 mol% of Ti while octahedrally coordinated Ti predominated in the high Ti content region (Ti $\geqslant$ 50 mol%). Tetrahedral Ti species catalyse the epoxidation of oct-1-ene and cyclohexene using *tert*-butyl hydroperoxide as an oxidant. Lewis acid sites of the titania–silica also originated from the tetrahedral Ti species. Both epoxidation activity and Lewis acidity of the titania–silica were well explained by the coordinative unsaturation of the tetrahedral Ti site.

Titania–silica mixed oxides have attracted much attention as ceramic glasses and catalysts. Sakka and Kamiya prepared titania–silica glasses by a sol–gel method starting from the corresponding metal alkoxides.[1] This method provides glasses in various forms such as fibres, thin films and bulk glasses.[2] Many other reports deal with the effect of Ti in titania–silica glasses on their performance.[3–8] Titania–silica also serves as a catalyst. It is a well known solid acid, catalysing the isomerization of butenes,[7] cumene dealkylation, propan-2-ol dehydration[8] *etc.* In contrast to other solid acids, it contains a transition-metal oxide, TiO_2, which can promote oxidation reactions such as carbon monoxide oxidation and the photo-oxidation of methane and propene.[9–11] The advantage of the combination of the oxidizing ability of Ti with the acidity of titania–silica was well demonstrated for the decomposition of 1,2-dichloroethane.[12] Although most acid catalysts were deactivated during the reaction owing to coke formation, TiO_2 eliminated the coke by combustion and maintained the activity of titania–silica. As the nature of titania–silica depends very much on the state of the Ti in it, many investigations have been carried out to elucidate the microstructural configurations of Ti.[1–4,6,13–15] The proposed structures are: segregated TiO_2, tetrahedral Ti, octahedral Ti, amorphous anatase-like TiO_2 *etc.* Greegor *et al.* reported that a decrease in the Ti content resulted in an increase in the ratio of tetrahedral Ti to octahedral Ti.[4] However, the relationship between the Ti configuration and the catalytic action of titania–silica has not been investigated. The cause of the acidity of titania–silica is also controversial. Tanabe *et al.* proposed that the acidity is induced by a charge imbalance due to the difference in the coordination states of Ti^{4+} and Si^{4+}.[16] Nishiwaki *et al.* reported that a decrease in the particle size of TiO_2 leads to a charge imbalance, inducing acid sites even in the absence of silica.[17]

In this work the microstructural configuration of Ti has been investigated by an EXAFS technique combined with IR analysis to elucidate the active catalytic site in titania–silica. Liquid-phase epoxidation of oct-1-ene and cyclohexene with *tert*-butyl hydroperoxide was employed as a test reaction. The acid nature of titania–silica was also discussed.

Experimental

Materials

Ba_2TiO_4, a standard sample for tetrahedral Ti, was prepared by thoroughly mixing $BaCO_3$ and anatase-type TiO_2 (Ba/Ti molar ratio of 2), followed by calcination in a platinum crucible at 1473 K for 24 h.[18] Other standard Ti samples were obtained commercially. Silica gel was provided by the Catalysis Society of Japan. Benzene was dried over calcium chloride, refluxed with sodium metal overnight and then distilled. Oct-1-ene and pyridine were dried with calcium sulfate and sodium hydroxide, respectively. Hammett indicators, *tert*-butyl hydroperoxide (TBHP), cyclohexene and other reagents were obtained commercially and used without further purification.

Preparation of Titania–Silica

Titania–silica with a known Ti content was prepared by a rapid sol–gel method.[12] Known amounts of tetraisopropyl titanate(IV) and tetraethyl orthosilicate (total amount of Ti and Si 0.2 mol) were dissolved in 40 cm^3 of ethanol and stirred for 30 min at room temperature, then refluxed at 353 K for 30 min. After the solution was cooled to room temperature, a mixture of ethanol (40 cm^3) and 0.01 mol dm^{-3} aqueous acetic acid (100 cm^3) was added to this solution over *ca.* 5 min with vigorous stirring. The solution containing the resultant precipitate was again refluxed at 353 K for 1 h. The mixture was then kept standing at 353 K until no weight change was observed (*ca.* 1 week). The titania–silica obtained was calcined at 823 K in air for 3 h.

Apparatus and Procedure

Epoxidation of oct-1-ene and cyclohexene was carried out as follows. A chlorobenzene solution of 0.2 mol dm^{-3} cyclohexene (10 cm^3) [or neat oct-1-ene (10 cm^3)] and 0.2 g of titania–silica was placed in a 50 cm^3 three-necked flask. The flask was purged with nitrogen and immersed in an oil bath kept at 363 K, and 0.2 cm^3 of a benzene solution of TBHP (50 wt.%) was added (concentration: 0.1 mol dm^{-3}). The

solution was stirred with a magnetic agitator, and the reaction was followed by analysing the remaining TBHP and the epoxides produced. The selectivity of epoxidation was defined by the ratio of the amount of epoxide formed to the amount of TBHP consumed.

Analysis

1,2-Epoxyoctane was determined by a Shimadzu GC-3BT gas chromatograph with a Chromosorb 101 column (3 m) at 393 K. 1,2-Epoxycylohexane was similarly determined with a column of 20% PEG 20M plus 5% KOH on Celite 545 (3 m). The amount of epoxides was also determined according to the hydrochloric acid–pyridine method on the basis of the amount of hydrochloric acid consumed by epoxide.[19]

The acid strength and the amount of acid sites of the titania–silica were measured in dry benzene by using the following Hammett indicators: Methyl Red ($pK_a = 4.8$), Methyl Yellow ($pK_a = 3.3$), benzeneazodiphenylamine ($pK_a = 1.5$), dicinnamalacetone ($pK_a = -3.0$), benzalacetophenone ($pK_a = -5.6$) and anthraquinone ($pK_a = -8.2$).

Titania–silica was oxidized with 8 kPa of oxygen at 673 K for 2 h and then sealed into a Q-pack pouch in a dry box for the X-ray absorption measurements. The absorption spectra were obtained at the beam line 6B and 7C stations of the Photon Factory in the National Laboratory for High Energy Physics (Tsukuba) with a ring energy of 2.5 GeV and a ring current of 150 – 250 mA. An Si(111) double crystal was used to monochromatize the X-rays. The spectra were recorded both by fluorescence and transmission techniques at room temperature over the range of photon energies from 4.7 to 6.0 KeV for the Ti K-edge (resolution energy of 0.5 eV at the edge). The data analysis method has been described elsewhere.[20–22]

Ammonia adsorbed on titania–silica was analysed with a JEOL JIR-6500W FTIR spectrophotometer with a diffuse reflectance attachment. Titania–silica was diluted to 5 wt.% with KBr powder.

Electron spectroscopy for chemical analysis (ESCA) was carried out with a Shimadzu ESCA 750 spectrophotometer.

Results and Discussion

Table 1 shows the BET surface area, surface Ti content, and acid strength (expressed by Hammett acidity function H_0) of the titania–silica samples used in this work. The surface area first decreases on incorporation of Ti into SiO_2, then increases at 30 to 50 mol% of Ti, before decreasing at higher Ti content. The reason for this irregular change in the surface area is not yet known. ESCA analysis showed that the surface Ti content is less than that in the bulk for almost all titania–silica samples. Stakheev *et al.* also observed the same phenomenon for titania–silica prepared by the co-precipitation method.[23] Although single-component TiO_2 and SiO_2 exhibited only weak acid strength ($3.3 < H_0 \leqslant 4.8$), the combination of both oxides produced stronger acid sites.

Table 1 Properties of titania–silica

Ti (mol%)	S^a/ $m^2\ g^{-1}$	surface Ti (mol%)	acid strength[b] (H_0)
0	499.6	0	$3.3 < H_0 \leqslant 4.8$
5	459.0	5.3	$-5.6 < H_0 \leqslant -3.0$
10	330.2	7.1	$-5.5 < H_0 \leqslant -3.0$
20	222.2	10.7	$-5.6 < H_0 \leqslant -3.0$
30	181.8	14.8	$-8.2 < H_0 \leqslant -5.6$
40	258.1	26.9	$-8.2 < H_0 \leqslant -5.6$
50	291.1	38.5	$-8.2 < H_0 \leqslant -5.6$
60	238.8	51.4	$-8.2 < H_0 \leqslant -5.6$
75	204.2	61.3	$-8.2 < H_0 \leqslant -5.6$
100	32.8	100	$3.3 < H_0 \leqslant 4.8$

[a] BET surface area. [b] Expressed by Hammett acidity function H_0.

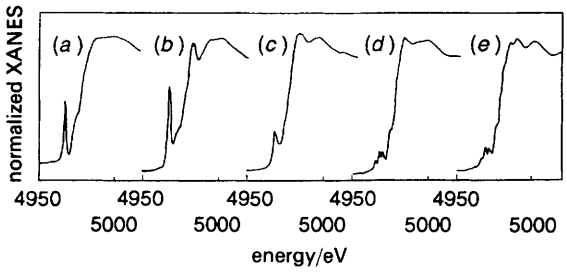

Fig. 1 XANES spectra of standard samples: (*a*) $Ti(OPr^i)_4$, (*b*) Ba_2TiO_4, (*c*) $Ti(OBu^n)_4$, (*d*) TiO_2 (anatase), (*e*) TiO_2 (rutile)

XANES Spectra of Standard Ti Samples

X-Ray absorption near-edge structure (XANES) spectra of various Ti-containing standard samples are shown in Fig. 1. Titanium(IV) isopropoxide [$Ti(OPr^i)_4$] and Ba_2TiO_4, which have tetrahedrally coordinated Ti, show one sharp pre-edge peak. This absorption peak is due to a transition from the 1s level to the 3d level of metal ions. Although the transition is formally forbidden, asymmetrical configurations of metal ions allow it. The intensity (area) of the peak increases as the configuration of the metal ion deviates from octahedral symmetry.[24] Ba_2TiO_4 has an almost regular tetrahedral structure (average Ti—O bond length: 1.808 Å).[25] The pre-edge peak for titanium(IV) *n*-butoxide [$Ti(OBu^n)_4$] is small and the Ti is located in a five-coordinate environment: it is reported that $Ti(OBu^n)_4$ is polymerized to five-coordinated Ti species.[26] The pre-edge peak of TiO_2 (both anatase- and rutile-types) which has an octahedral configuration [(1.937 Å × 4) + (1.964 Å × 2) and (1.946 Å × 4) + (1.984 Å × 2), respectively] shows a triplet. Uozumi *et al.* analysed the triplet taking dipole and quadrupole transitions into consideration.[27] Thus the shape and intensity of the pre-edge peaks depend profoundly on the coordination states of Ti. The structures of Ti in the titania–silica were determined on the basis of their pre-edge peaks.

XANES Spectra of Titania–Silica with Different Ti Contents

XANES spectra of titania–silica samples with various compositions were obtained by the fluorescence method (Fig. 2). The result observed by the transmission method was almost the same although it is not shown in the figure. The spectra of Ti in the titania–silica with 40 mol% Ti or less have a tetrahedral feature like that in $Ti(OPr^i)_4$, while spectra similar to that of octahedral Ti in anatase-type TiO_2 were observed at high Ti content. However, the shapes of the pre-edge peaks of titania–silica with 50 and 60 mol% of Ti are not exactly identical to that of TiO_2. This seems to show that tetrahedral Ti and octahedral Ti are mixed in these titania–silica samples. Although we attempted the deconvolution of these peaks into the corresponding elements from octahedral Ti and tetrahedral Ti by assuming that there were four peaks, it was unsuccessful. Thus Table 2 shows the result of the simple deconvolution analysis of these peaks on the assumption that the XANES spectra of the titania–silica samples with no more than 40 mol% Ti have a singlet, and a triplet was observed only for the samples with more than 40 mol% Ti. The position of each peak was expressed by its relative deviation from the inflection point of the continuum. As the singlet for the sample with 40 mol% of Ti and below was assumed to be due to tetrahedral Ti species, it was designated as peak T_d. The strongest peak in the triplet for the titania–silica with 50 to 75 mol% of Ti is the second peak. This peak

Table 2 Pre-edge peak of titania–silica measured by fluorescence method

Ti (mol%)	position[a] /eV	width /eV	height[b]	area[b]
5	−12.8	2.05	0.21	0.67
10	−12.13	1.86	0.23	0.68
20	−11.83	2.06	0.22	0.71
30	−11.82	1.76	0.23	0.64
40	−11.60	2.06	0.19	0.60
	−12.84	0.93	0.04	0.06
50	−11.15	1.77	0.09	0.25
	−8.51	1.65	0.04	0.09
	−12.81	1.09	0.06	0.10
60	−10.82	1.78	0.16	0.45
	−8.38	2.51	0.07	0.29
	−12.70	1.04	0.04	0.07
75	−10.96	1.72	0.09	0.28
	−8.58	2.02	0.05	0.16
	−12.57	1.11	0.05	0.08
100	−10.26	2.10	0.13	0.43
	−7.71	2.62	0.10	0.43

[a] Relative to the inflection point of the continuum. [b] Arbitrary unit.

is at a lower position than the corresponding second peak of TiO_2. Thus even the triplet of the sample with high Ti content is still influenced by the presence of peak T_d. The relative amount of tetrahedral Ti as estimated by the area of peak T_d takes a maximum at Ti content 20 mol%. Greegor *et al.* observed the same phenomenon for the XANES spectra of titania–silica glass prepared by flame hydrolysis.[4] They explained the decrease in the tetrahedral Ti peak at very low Ti contents as due to the fission of the oxygen bridge of the SiO_2 unit by TiO_2 to form two terminal oxygens and an octahedral Ti species.

EXAFS Spectra of Ti K-Edge

Fig. 3 shows the Fourier transforms of k^3-weighted EXAFS spectra at the Ti K-edge measured in transmission mode. The phase shift correction was not applied. The spectra are almost the same for titania–silica with ⩽40 mol% Ti. Each has a sharp peak which is attributed to the Ti—O bond. No additional peak is observed for samples with ⩽20 mol% Ti. A small peak is observed in the second shell (2.8 Å) for the 40 mol% Ti sample. For samples with ⩾50 mol% Ti, the first-shell peak shifts to a longer position and an additional second-shell peak clearly appears which corresponds to the Ti–O–Ti interaction. The positions of both peaks are almost the same as those of anatase-type TiO_2 although their relative intensities are different. These results are compatible with the result of XANES analysis that the samples with less than 40 mol% Ti have tetrahedral Ti and octahedral Ti predominates above 40 mol% Ti.

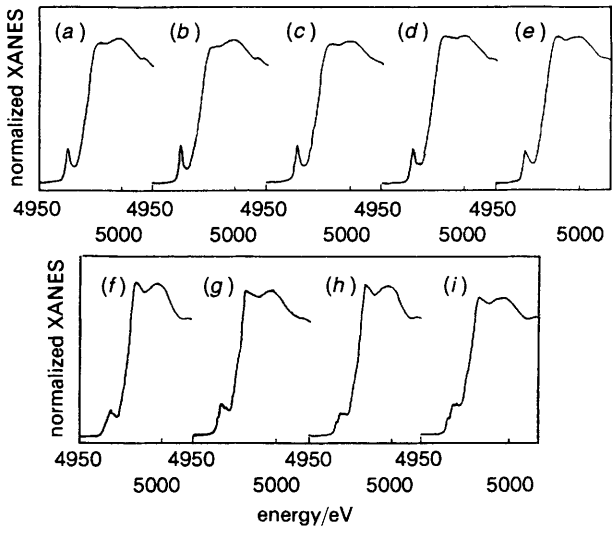

Fig. 2 XANES spectra of titania–silica samples measured by the fluorescence method: Ti/Si atomic ratio: (*a*) 5/95, (*b*) 10/90, (*c*) 20/80, (*d*) 30/70, (*e*) 40/60, (*f*) 50/50, (*g*) 60/40, (*h*) 75/25, (*i*) 100/0

To obtain more information about the structures of Ti, analyses of EXAFS oscillations were carried out with a curve-fitting method based on single-scattering theory:[22]

$$\chi(k) = \sum_j (N_j S_j / k r_j^2) F_j(k) \exp(-2\sigma_j^2 k^2) \times \exp(-2r_j/\lambda) \sin\{2kr_j + \delta_j(k)\} \quad (1)$$

where N_j is the coordination number of the jth shell at the distance R_j from the X-ray absorbing atom, $F_j(k)$ the back-scattering amplitude for the photoelectron wavenumber k, S_j the damping factor for compensation of the loss by inelastic scattering, δ_j the phase shift, σ_j the Debye–Waller factor and λ the mean free path of the photoelectron. Back-scattering amplitude and phase-shift parameters tabulated by Teo and Lee[28] were not applicable. Therefore, their parameters for the Ti—O bond were extracted from the EXAFS oscillation of $Ti(OPr^i)_4$ for which the bond distance and coordination number are taken as 1.76 Å and 4, respectively.

Curve fitting was carried out for the peaks of the first shell in the region of 0.6–2.0 Å of Fourier transforms in Fig. 3 (Table 3). One-shell fitting was applied for anatase-TiO_2 since the bond distances [1.934 Å (4) and 1.980 Å (2); the numbers in parentheses are the coordination numbers][29] are too close. An example of curve fitting is shown for titania–silica with 5 mol% Ti in Fig. 4. The calculated values of the bond distance and coordination number are in fairly good agreement with the reference data. Bond distances of titania–silica with ⩽20 mol% Ti are close to those of tetrahedral compounds: similar to that of Ba_2TiO_4 (average 1.808 Å)[25] and a little larger than that of $Ti(OPr^i)_4$. The coordination number of the

Table 3 Structural-parameters for Ti—O bonds in the first shell of titania–silica mixed oxides

Ti (mol%)	bond length/Å	coordination number[a]	Debye–Waller factor/Å^2	ΔE_0	R factor[b] (%)
5	1.79	4.02	0.00546	−5.6	4.5
10	1.79	4.09	0.00390	−1.4	5.0
20	1.80	4.36	0.00663	−1.4	4.8
40	1.83	4.31	0.01005	−1.5	4.7
50	1.89	5.01	0.00595	−0.3	4.5
$Ti(OPr^i)_4$	1.76	4.00	—	−3.5	—
TiO_2 (anatase)	1.92	5.99	0.00418	0.0	5.3

[a] The coordination number is estimated on the basis that the coordination number of the Ti—O bond of $Ti(OPr^i)_4$ is 4.00. [b] $R = \{\sum [\chi_{obs}(k) - \chi_{calc}(k)]^2 / \sum [\chi_{obs}(k)^2]\}^{1/2}$.

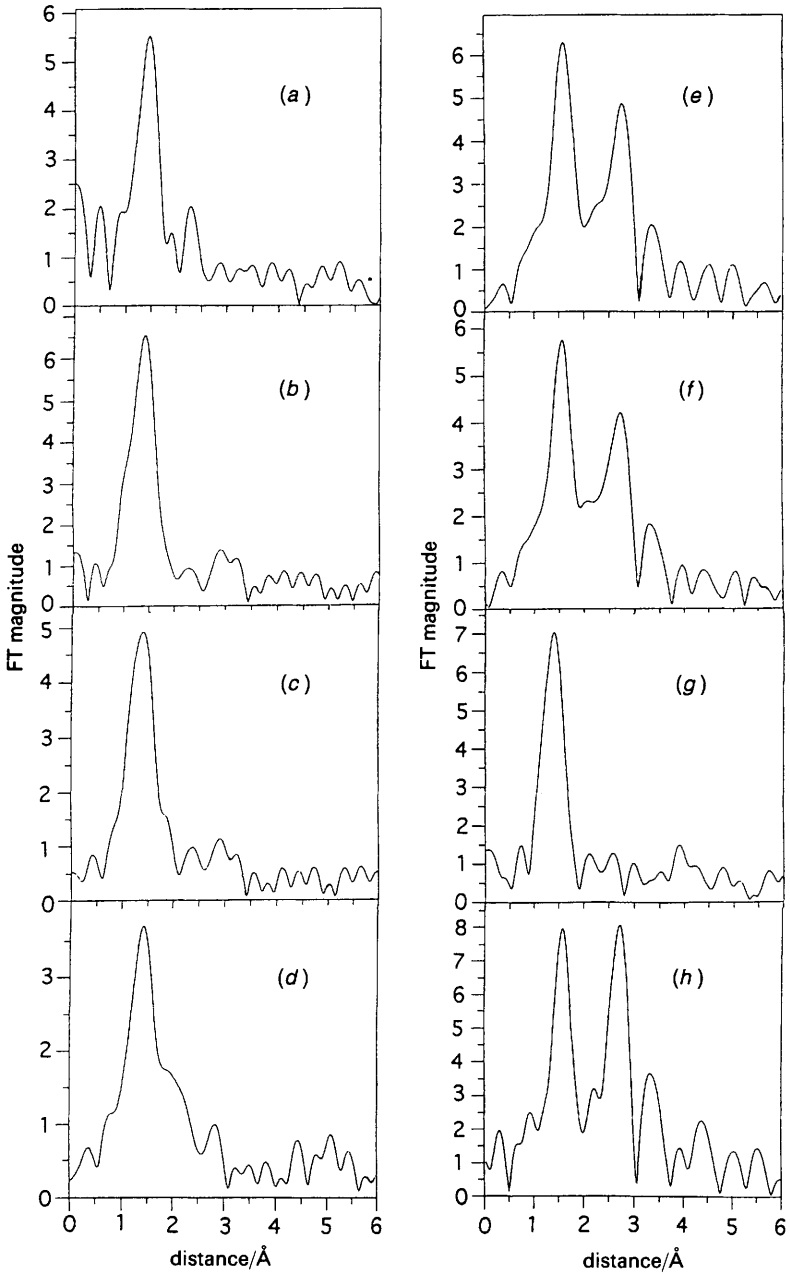

Fig. 3 Fourier transforms of k^3-weighted EXAFS spectra: Ti/Si atomic ratio (*a*) 5/95, (*b*) 10/90, (*c*) 20/80, (*d*) 40/60, (*e*) 50/50, (*f*) 75/25, (*g*) $Ti(OPr^i)_4$, (*h*) TiO_2 (anatase)

Ti—O bond in the samples with 5 and 10 mol% Ti is *ca.* 4. Therefore, titanium species in titania–silica of low Ti content are in a tetrahedral structure with an equivalent Ti—O bond which is very similar to that of titania–silica prepared by a sol–gel method[30] or flame hydrolysis[4] and that of titanium silicalite,[31] although there are still many arguments on the precise structure of the latter.[32] The Ti—O bond distance increases with the increase in the Ti content over the range 5–50 mol% Ti. The bond elongation is due to the mixing of an octahedral structure. This is supported by the fact that the coordination number also increases from 4 to 5. The intermediate coordination number for the titania–silica with 50 mixing of tetrahedral and octahedral structures, which reflects the complex XANES spectrum.

X-Ray absorption analysis shows that a distinct structural change occurs in the region of 40–50 mol% Ti. Anatase-TiO_2 crystallites are formed above 50 mol% Ti as was indicated by X-Ray diffraction analysis.[33]

IR of Ammonia adsorbed on Titania–Silica

IR spectra were observed for ammonia adsorbed on titania–silica in order to investigate its acid nature. Titania–silica was pretreated at 373 K for 1 h *in vacuo* before the introduction of ammonia. All samples showed two absorption bands at 1420 and 1605 cm^{-1} (Fig. 5). The first was assigned to an ammonium ion adsorbed on a Brønsted acid site.[34] The effect of the pretreatment temperature on the intensity of these two bands is shown in Fig. 6. As the temperature increases, the intensity of the band at 1605 cm^{-1} increases, whereas the band at 1420 cm^{-1} becomes small. Primet *et al.* reported that TiO_2 loses its surface OH group on heating to form coordinatively unsaturated Ti^{4+} species responsible for Lewis acid sites.[35] Thus the absorption band at 1605 cm^{-1} was assigned to the stretching mode of the ammonia adsorbed on Lewis acid sites of titania–silica.[36] Silica alone showed no absorption band at 1605 cm^{-1}: Lewis acidity is produced by Ti

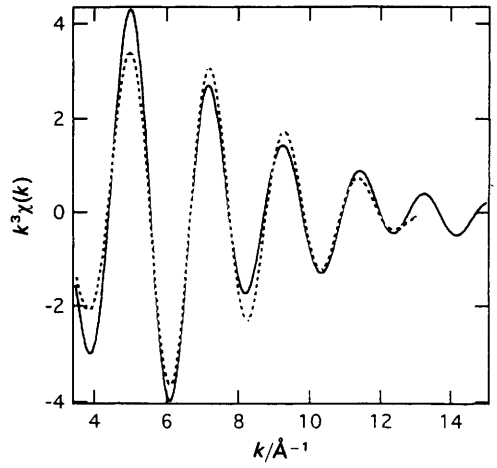

Fig. 4 Simulation of the EXAFS oscillation of the first-shell Ti—O bond (Fig. 3) of the titania–silica sample with Ti/Si atomic ratio 5/95. (——) Experimental, (– – –) simulated.

species. It is interesting to see that the change in the Ti content affects the ratio of the intensity of the absorption band of ammonia on Lewis acid sites to that on Brønsted acid sites: the relative absorption-band intensity of ammonia on Lewis acid sites seems to be larger for titania–silica with lower Ti content. Thus the relationship between the amount of Lewis acid sites and Ti content was analysed as shown below and the result is exhibited in Fig. 7. Since the Lewis acid sites originate from Ti species, the amount of Lewis acid sites is normalized per unit amount of surface Ti; that is, the area of the absorption band at 1605 cm^{-1} is divided by the surface amount of Ti measured by ESCA.[33] (Table 1). Thus $area_L$ (in arbitrary units) on the ordinate indicates the ratio of the amount of Ti exhibiting Lewis acidity to the total amount of surface Ti. Fig. 7 also shows the relationship between the Ti content and the area of peak T_d (that is, the amount of tetrahedral Ti shown in Table 2). As the Ti content decreases, the amount of tetrahedral Ti increases and reaches a maximum at 10–20 mol% Ti. Since the peak T_d could not be

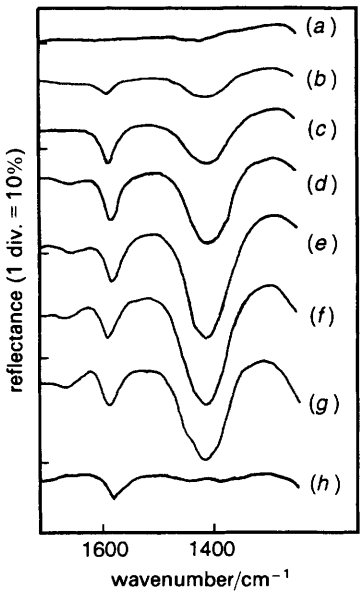

Fig. 5 IR spectra of ammonia adsorbed on titania–silica: Ti/Si atomic ratio: (*a*) 0/100, (*b*) 5/95, (*c*) 10/90, (*d*) 20/80, (*e*) 40/60, (*f*) 60/40, (*g*) 75/25, (*h*) 100/0. Titania–silica was pretreated at 373 K *in vacuo* for 1 h before the introduction of 400 Pa of ammonia for 10 min at the same temperature. IR measurements were carried out at 373 K after evacuation of excess ammonia.

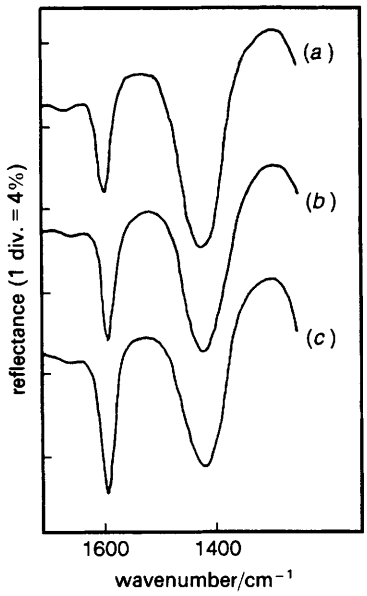

Fig. 6 Effect of the pretreatment temperature on the IR spectra of ammonia adsorbed on titania–silica (Ti/Si atomic ratio = 20/80): pretreatment temperature: (*a*) 373, (*b*) 523 and (*c*) 673 K. Other procedures are the same as for Fig. 4.

separated in the spectra of titania–silica with ⩾50 mol% Ti, the amount of tetrahedral Ti was expediently set as zero at high Ti contents. The amount of Lewis acid sites also increases with the decrease in Ti content to a maximum at 10–20 mol% Ti. The coincidence in the behaviour of both curves clearly shows that the tetrahedral Ti species is responsible for the Lewis acid sites in titania–silica owing to its coordinatively unsaturated nature. Odenbrand *et al.* also reported that the tetrahedral Ti species in titania–silica is the cause of its Lewis acidity.[37]

Epoxidation of Oct-1-ene and Cyclohexene

The results of the epoxidation of oct-1-ene and cyclohexene are shown in Table 4. The composition of titania–silica also affected the epoxidation ability; the selectivity is high on the titania–silica samples with 10–20 mol% Ti. This situation is more clearly demonstrated in Fig. 8. As the Ti content decreases, the selectivity increases to a maximum at Ti content 10–20 mol%. The selectivity curves, especially that for 1,2-epoxycyclohexane, coincide well with the curve showing the change in the amount of tetrahedral Ti species. Thus tetrahedral Ti is surely the active site for the epoxida-

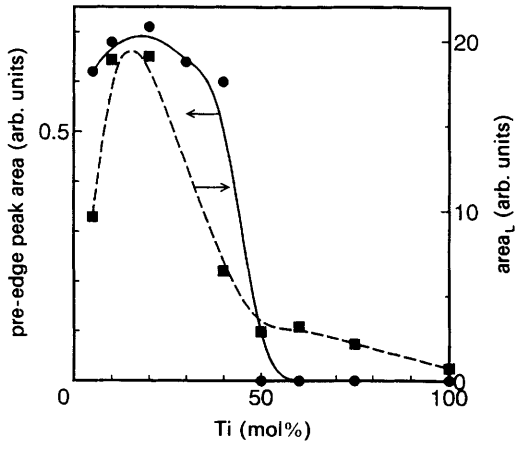

Fig. 7 Pre-edge peak area and the amount of Lewis acid sites *vs.* Ti content: (——) pre-edge area, (– – –) the amount of Lewis acid sites

Table 4 Epoxidation on titania–silica[a]

	1,2-epoxyoctane		1,2-epoxycyclohexane	
Ti (mol%)	yield[b]	selectivity[c]	yield[b]	selectivity[c]
0[d]	6.5	30.1	—	—
5	66.5	70.0	22.5	45.0
10	73.6	76.3	37.3	51.1
20	50.0	53.3	46.4	65.0
30	38.1	40.0	39.0	55.5
40	20.9	21.8	34.3	43.0
50	12.2	12.5	19.3	25.0
60	3.4	3.5	10.3	11.4
75	0	0	4.1	8.7
100	0	0	1.1	7.0

[a] Reaction conditions are described in the Experimental section. The reactions were carried out for 6 h (oct-1-ene) and for 7 h (cyclohexene). [b] Yield is based on the amount of TBHP charged. [c] Selectivity is defined by the ratio of epoxides formed to TBHP decomposed. [d] Standard catalyst provided by the Catalysis Society of Japan.

tion of alkenes. It is well known that epoxidation of alkenes proceeds *via* a non-radical step where the hydroperoxide (oxidant) must be first coordinated to vacant sites of the metal ions (Lewis acid sites) to give an electrophilic character before attacking the alkenic double bond with its atomic oxygen.[38] Thus the coordinative unsaturation of the tetrahedral Ti species in titania–silica is clearly responsible for the epoxidation reaction. When octahedral Ti species predominate, coordination of TBHP would be impossible, and, in turn, radical decomposition of TBHP on TiO_2 would occur leading to the decrease in selectivity.[33]

The salient findings in this work are as follows: When the Ti content in titania–silica is high ($\geqslant$50 mol%), Ti is present mainly in an octahedral configuration. With decrease in Ti content, the tetrahedral configuration appears in an isolated state in the tetrahedral SiO_2 matrix. This coordinatively unsaturated tetrahedral Ti shows interesting catalytic and physical properties, *i.e.* it produces Lewis acid sites that act as active sites for the epoxidation reaction.

This work was performed under the approval of the Photon Factory Program Advisory Committee of National Institute of High Energy Physics (Proposal No. 93G15). The authors are indebted to Prof. Nomura and Mr. Koyama of KEK-PF of Tsukuba for the X-ray measurements. They are also grateful to Dr. T. Tanaka of Kyoto University for permission to use his XANES analysis program. The simulation was carried out with FACOM M780/30 computer in the Data Processing Center at Kyoto University. H.K. acknowledges support of this research by a Grant-in-Aid from the Ministry of Education, Science, and Culture, Japan.

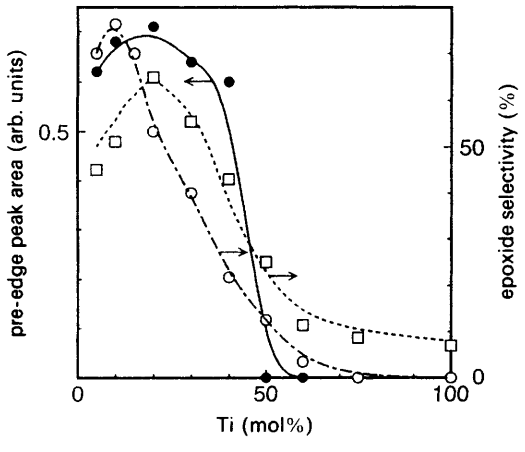

Fig. 8 Pre-edge peak area and epoxide selectivity *vs.* Ti content: (——) pre-edge peak area, (– – –) selectivity to 1,2-epoxycyclohexane, (– – –) selectivity to 1,2-epoxyoctane

References

1 S. Sakka and K. Kamiya, *J. Non-Cryst. Solids*, 1980, **42**, 403.
2 K. Kamiya and S. Sakka, *Nippon Kagaku Kaishi*, 1981, 1571.
3 D. R. Sandstrom, F. W. Lytle, P. S. P. Wei, R. B. Greegor, J. Wong and P. Schultz, *J. Non-Cryst. Solids*, 1980, **41**, 201.
4 R. B. Greegor, F. W. Lytle, D. R. Sandstrom, J. Wong and P. Schultz, *J. Non-Cryst. Solids*, 1983, **55**, 27.
5 M. F. Best and R. A. Condrate Sr., *J. Mater. Sci. Lett.*, 1985, **4**, 994.
6 S. M. Mukhopadhyay and S. H. Garofalini, *J. Non-Cryst. Solids*, 1990, **126**, 202.
7 H. Hattori, M. Itoh and K. Tanabe, *J. Catal.*, 1975, **38**, 172.
8 J. R. Sohn and H. J. Jang, *J. Catal.*, 1991, **132**, 563.
9 Y. Onishi and T. Hamamura, *Bull. Chem. Soc. Jpn.*, 1970, **43**, 996.
10 K. R. Thampi, J. Kiwi and M. Graetzel, *Catal. Lett.*, 1988, **1**, 109.
11 M. Anpo, H. Nakaya, S. Kodama, Y. Kubokawa, K. Domen and T. Onishi, *J. Phys. Chem.*, 1986, **90**, 1633.
12 S. Imamura, H. Tarumoto and S. Ishida, *Ind. Eng. Chem. Res.*, 1989, **28**, 1449.
13 G. A. Waychunas, *Am. Mineral.*, 1987, **72**, 89.
14 C. U. I. Odenbrand, S. L. T. Andersson, L. A. H. Andersson, J. M. G. Brandin and G. Busca, *J. Catal.*, 1990, **125**, 541.
15 K. Asakura, J. Inukai and Y. Iwasawa, *J. Phys. Chem.*, 1992, **96**, 829.
16 K. Tanabe, T. Sumiyoshi, K. Shibata, T. Kiyoura and J. Kitagawa, *Bull. Chem. Soc. Jpn.*, 1974, **47**, 1064.
17 K. Nishiwaki, N. Kakuta, A. Ueno and H. Nakabayashi, *J. Catal.*, 1989, **118**, 498.
18 J. J. Ritter, R. S. Roth and J. E. Blendell, *J. Am. Ceram. Soc.*, 1986, **69**, 155.
19 K. Kimura, in *Bunseki Kagaku Benran*, Maruzen, Tokyo, 1981, p. 334.
20 S. Yoshida, T. Tanaka, T. Hanada, T. Hiraiwa, H. Kanai and T. Funabiki, *Catal. Lett.*, 1992, **12**, 277.
21 H. Kanai, H. Mizutani, T. Tanaka, T. Funabiki, S. Yoshida and M. Takano, *J. Mater. Chem.*, 1993, **2**, 703.
22 T. Tanaka, H. Yamashita, R. Tsuchitani, T. Funabiki and S. Yoshida, *J. Chem. Soc., Faraday Trans. 1*, 1988, **84**, 2987.
23 A. Y. Stakheev, E. S. Shpiro and J. Apijok, *J. Phys. Chem.*, 1993, **97**, 5668.
24 F. W. Kutzler, C. R. Natoli, D. K. Misemer, S. Doniach and K. O. Hodgson, *J. Chem. Phys.*, 1980, **73**, 3274.
25 K. K. Wu and I. D. Brown, *Acta Crystallogr., Sect. B*, 1973, **29**, 2009.
26 F. Babonneau, S. Doeuff, A. Leaustic, C. Sanchez, C. Cartier and M. Verdaguer, *Inorg. Chem.*, 1988, **27**, 3166.
27 T. Uozumi, K. Okada, A. Kotani, O. Durmeyer, J. P. Kappler, E. Beaurepaire and J. C. Parlebas, *Europhys. Lett.*, 1992, **18**, 85.
28 B. K. Teo and P. A. Lee, *J. Am. Chem. Soc.*, 1979, **101**, 2815.
29 A. F. Wells, in *Structural Inorganic Chemistry*, Clarendon Press, Oxford, 5th edn., 1984, p. 541.
30 Z. Liu and R. J. Davis, *J. Phys. Chem.*, 1994, **98**, 1253.
31 S. Bordiga, F. Boscherini, S. Coluccia, F. Genoni, C. Lamberti, G. Leofanti, L. Marchese, G. Petrini, G. Vlaic and A. Zecchina, *Catal. Lett.*, 1994, **26**, 195.
32 D. Trong On, A. Bittar, A. Sayari, S. Kaliaguine and L. Bonneviot, *Catal. Lett.*, 1992, **16**, 85 and references cited therein; A. Jentys and C. R. A. Catlow, *Catal. Lett.*, 1993, **22**, 251.
33 S. Imamura, S. Ishida, H. Tarumoto, Y. Saito and T. Ito, *J. Chem. Soc., Faraday Trans.*, 1993, **89**, 757.
34 J. J. Dines, C. H. Rochester and A. W. Ward, *J. Chem. Soc., Faraday Trans.*, 1991, **87**, 643.
35 M. Primet, P. Pichat and M. V. Mathieu, *J. Phys. Chem.*, 1971, **75**, 1221.
36 S. Coluccia, S. Lavagnino and L. Marchese, *J. Chem. Soc., Faraday Trans. 1*, 1987, **87**, 477.
37 C. U. I. Odenbrand, J. G. M. Brandin and G. Busca, *J. Catal.*, 1992, **135**, 505.
38 M. N. Sheng and J. G. Zajacek, *J. Org. Chem.*, 1970, **35**, 1839.

Paper 4/05312E; *Received* 31*st August*, 1994